Tuberculosis 114 (2019) 9–16

Contents lists available at ScienceDirect

Tuberculosis

journal homepage: www.elsevier.com/locate/tube

Molecular Aspects

Interactions of domain antibody (dAbκ11) with *Mycobacterium tuberculosis* Ac_2SGL in complex with CD1b

Cheh Tat Law[a], Frank Camacho[b], Luis F. Garcia-Alles[c], Martine Gilleron[d], Maria E. Sarmiento[e], Mohd Nor Norazmi[e], Armando Acosta[e,**], Yee Siew Choong[a,*]

[a] Institute for Research in Molecular Medicine (INFORMM), Universiti Sains Malaysia, Minden, Malaysia
[b] Biologicals Sciences School, University of Conception, Chile
[c] LISBP, INSA, University of Toulouse, Toulouse Cedex, France
[d] Institut de Pharmacologie et Biologie Structurale, Université de Toulouse, Toulouse, France
[e] School of Health Sciences, Health Campus, Universiti Sains Malaysia, Kubang Kerian, Malaysia

ARTICLE INFO

Keywords:
Ac_2SGL
Mycobacterium tuberculosis
Single domain antibody dAbκ11
Socking and molecular dynamics (MD) simulation
Binding free energy

ABSTRACT

Tuberculosis (TB) is the main cause of mortality among all infectious diseases. The presentation of lipids by CD1b molecules and the interactions of the CD1b-lipid complexes with the immune receptors are important for the understanding of the immune response to *Mycobacterium tuberculosis* (Mtb), and to develop TB control methods. A specific domain antibody (dAbk11) recognizing the complex of CD1b with Mtb sulphoglycolipid (Ac_2SGL) had been previously developed. In order to study the interactions of dAbk11 with Ac_2SGL:CD1b, the conformation of Ac_2SGL within CD1b was first modelled. The orientation of dAbκ11 with Ac_2SGL:CD1b was then predicted by a docking experiment and the complex was sampled using molecular dynamics simulation. Data showed that dAbκ11 Tyr32 O_H plays a decisive role in interacting with Ac_2SGL alkyl tail H_{O17}. The binding free energy calculation showed that Ac_2SGL establish strong hydrophobic interactions with dAbκ11. The model also predicted a higher affinity for the natural sulfoglycolipid (Ac_2SGL) than the synthetic analogue (SGL12), which was supported by the ELISA data. These results shed light on the likely mechanism of interactions between Ac_2SGL:CD1b and dAbκ11, thus making possible to envision the strategies for dAbκ11 optimization for possible future applications.

1. Introduction

Tuberculosis (TB) is the leading cause of mortality from infectious diseases [1–6]. One third of the human population is already infected with *Mycobacterium tuberculosis* (Mtb). This represents a huge reservoir of the microorganism with a high present and future impact as a source of new TB cases [1–6]. The current picture of the disease is characterized by absence of fully efficient diagnostic methods, the emergence of multidrug resistant TB strains (MDR-TB), ineffective therapeutic coverage, HIV co-infection and the unavailability of an effective vaccine [1–6]. A better knowledge of the mechanisms of pathogen action and of immune responses to Mtb are of paramount importance for the effective control of the TB pandemics, something that will rely on the development of new vaccines, diagnostics and therapies [7].

CD1b protein is a non-polymorphic transmembrane glycoprotein that is expressed associated with β_2-microglobulin on the surface of human antigen presenting cells (APC) [8]. Unlike major histocompatibility complex molecules (MHC) that present peptides to T cells, CD1b is able to present lipid and glycolipid antigens [9]. Ac_2SGL, a member of the acylated trehalose sulphate lipid family (SGL), is one of the antigens presented by CD1b molecules to T cells [10]. The Ac_2SGL:CD1b complex was shown to stimulate specific T cells from active or latently Mtb infected individuals, but not those from non-infected, or Bacillus Calmette-Guérin (BCG) vaccinated subjects [10]. It had been demonstrated that the number and type of acyl appendages on the trehalose decisively influence the strength of CD1b-dependent T cell responses [11]. In this regard, a few synthetic lipids that differed from the natural Ac_2SGL by the length and complexity of acyl appendages attached to the trehalose, were found to stimulate Ac_2SGL-specific T cells much like the natural antigen [11,12]. The structure of one of the most active synthetic molecules, SGL12, co-crystallised with human CD1b could be even elucidated (PDB id: 3T8X) [13]. In spite of this work, the antigenic

* Corresponding author.
** Corresponding author.
E-mail addresses: armando@usm.my (A. Acosta), yeesiew@usm.my (Y.S. Choong).

https://doi.org/10.1016/j.tube.2018.11.002
Received 3 July 2018; Received in revised form 26 October 2018; Accepted 2 November 2018

properties of the natural Ac_2SGL were never surpassed, especially in assays using APC, which demonstrated the importance of the fatty acyl structures of Mtb sulfoglycolipids on the capacity of stimulation of T cells [10,11].

Considering the importance of understanding how immune response to these Mtb lipids are triggered and the need to develop universal ligands for diagnosis of Mtb infections that are not affected by the antigen presenting molecules polymorphism, we have developed a light chain kappa domain antibody (dAbκ11). dAbκ11, developed using a synthetic human antibody library, is capable of efficiently recognizing the Ac_2SGL:CD1b complex [14].

In the present report, a molecular modelling approach was applied to study the interactions of dAbκ11 with Ac_2SGL:CD1b complex to highlight the residues that are likely important for the recognition of the Ac_2SGL:CD1b complex by dAbκ11. The model predicted a higher affinity with the natural sulfoglycolipid (Ac_2SGL) compared to its synthetic analogue (SGL12) that was further supported by ELISA results.

2. Methods

2.1. Starting structure of CD1b and lipids

The structure of CD1b in complex with the synthetic antigenic diacylsulfoglycolipid SGL12 and an endogenous spacer (PDB id: 3T8X; 1.9 Å resolution) was used as starting model for our work. In order to reduce the computational cost, however, only the antigen binding groove was used for the simulation, namely residues Phe 4 to Leu 181 of CD1b. Atoms from the bound endogenous spacer were also included for the simulations. On the other hand, the starting model for Mtb major Ac_2SGL acyl form (mol wt 1250; Fig. 1a) which is recognized by $CD8^+$ T cell clones [10], was built using Discovery Studio 3.0 [15] by editing the methyl-branches from the co-crystalized SGL12 in CD1b (ligand of PDB id: 3T8X; Fig. 1b) [13].

2.2. Docking of lipid into CD1b

The docking input files for lipids (Ac_2SGL & SGL12) and CD1b were prepared using AutoDockTools 4.2 [16]. The docking simulation was performed by Autodock Vina 1.1.2 [17] with default parameters. Gasteiger atomic point charges were assigned and the non-polar hydrogen atoms were merged. The number of rotatable bonds in lipids was set to the highest to enable full flexibility of the lipid alkyl tails. The grid spacing was set to 1.0 Å with a box size of $36 \times 34 \times 32$ $Å^3$ to include the binding groove of CD1b. In order to have a higher search space and to get the best conformation complex in the docking, 200 exhaustiveness flag was included for searching algorithm.

2.3. Molecular dynamics (MD) simulation of Ac2SGL:CD1b and SGL12:CD1b complex

The Ac_2SGL:CD1b and SGL12:CD1b complexes were further sampled by molecular dynamics (MD) simulation. The system was setup with standard Amber 12 protocol [18]. GAFF force field was assigned to the spacer, Ac_2SGL and SGL12, while AMBER ff14SB force field was used to assign atom types and charges to CD1b. Counter ions, Na^+, were added to neutralise the system. The complex was then solvated in a 10 Å octahedral TIP3P water box. A cut off distance of 8 Å was used for non-bonded interactions under periodic boundary condition. The time step was set to 1 fs and the trajectory was recorded every 0.1 ps. In minimization stage, 1000 steepest descent followed by 1000 conjugated gradient minimization steps were performed. In the first minimization, the backbones of the protein, lipids and spaces were restrained with

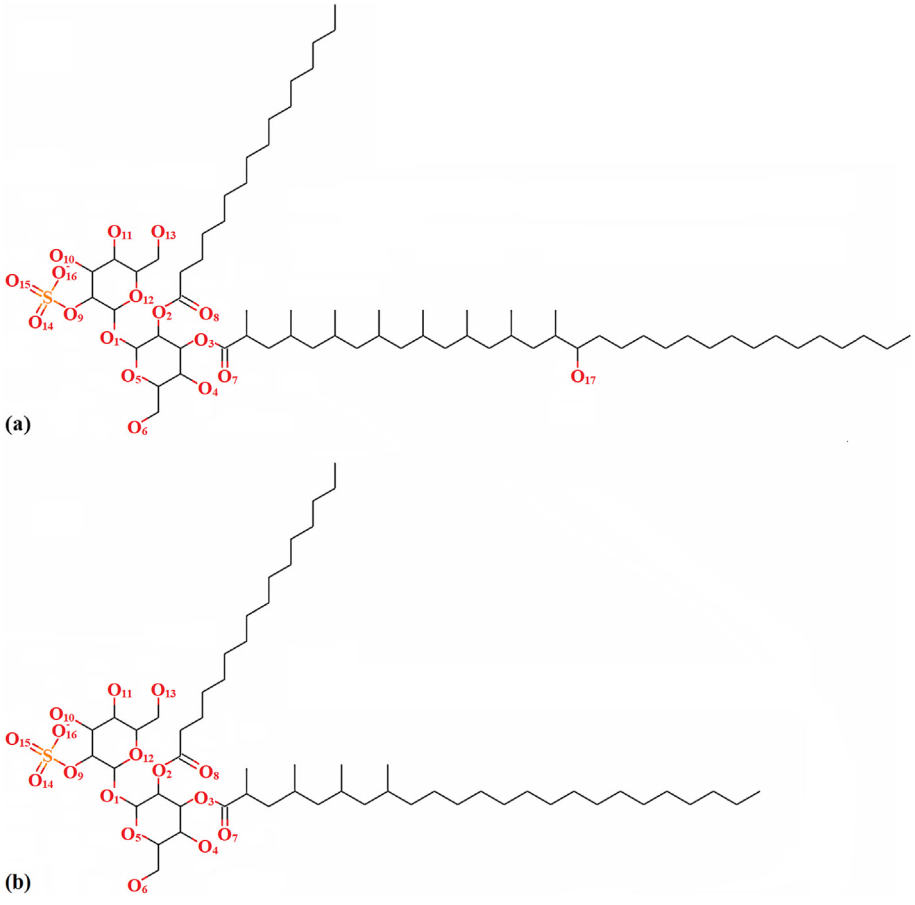

Fig. 1. The chemical structure of **(a)** Ac_2SGL and **(b)** SGL12.

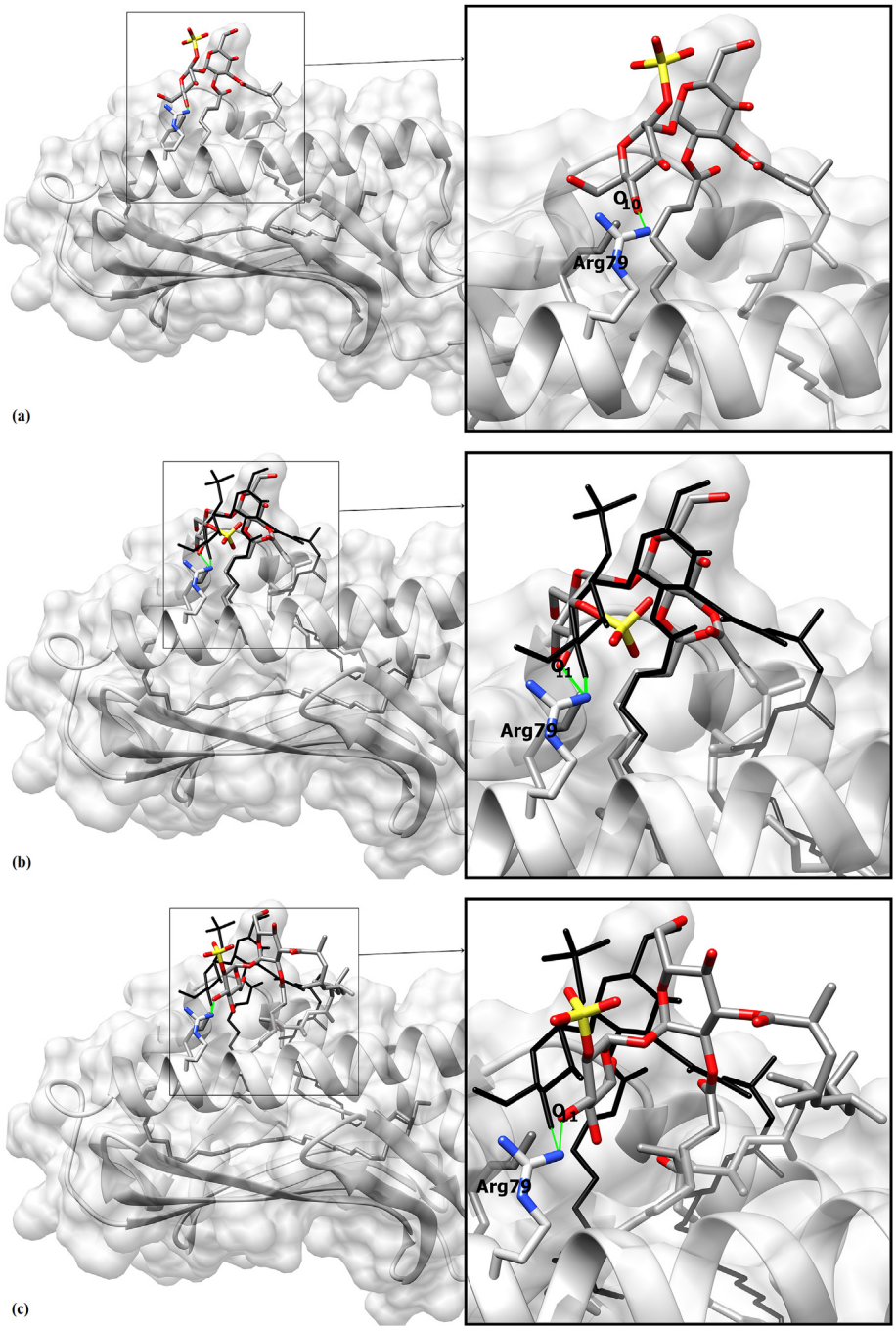

Fig. 2. Conformations of lipids in CD1b (ribbon and surface representation). **(a)** Crystal SGL12 (stick presentation coloured by atom type). **(b)** Crystal SGL12 (black stick) and conformation of docked SGL12 (stick presentation, coloured by atom type). **(c)** Crystal SGL12 (black stick) and conformation of docked Ac_2SGL (stick presentation, coloured by atom type). Grey stick is the spacer and green lines are hydrogen bonds between CD1b Arg79 with lipid. (For interpretation of the references to colour in this figure legend, the reader is referred to the Web version of this article.)

300 kcal/mol/Å^2 to relax the water molecules. The same number of minimization steps was repeated on unrestrained complex. Before production stage, the complex was gradually heated from 0 to 310 K within 20 ps by Langevin thermostat, while restrained with 100 kcal/mol/Å^2 for protein backbone, lipid, and spacer. A 0.5 ns unrestrained MD simulation was performed to obtain constant pressure with equilibrated density at 310 K. The MD simulation was carried out for 10 ns. A total of 500 snapshots from the last 0.5 ns of MD simulation were used to calculate the binding free energy of lipids (Ac_2SGL & SGL12) with CD1b.

2.4. Modelling of dAbκ11

The CDRs of dAbκ11 were identified by KABAT [19] and the BLAST [20] program was used to select the suitable immunoglobulin template for dAbκ11. For the comparative modelling of dAbκ11, template structural models were selected with the highest sequence identity coverage and resolution from the RCBS protein databank. The selected templates were a Vk domain of a human antibody (PDB id: 2BX5) [21] and a human antibody variable domain with increased aggregation resistance (PDB id: 3UPA) [22], presenting 95% and 93% identity to dAbκ11 sequence and resolutions of 2.7 Å and 1.8 Å, respectively. The

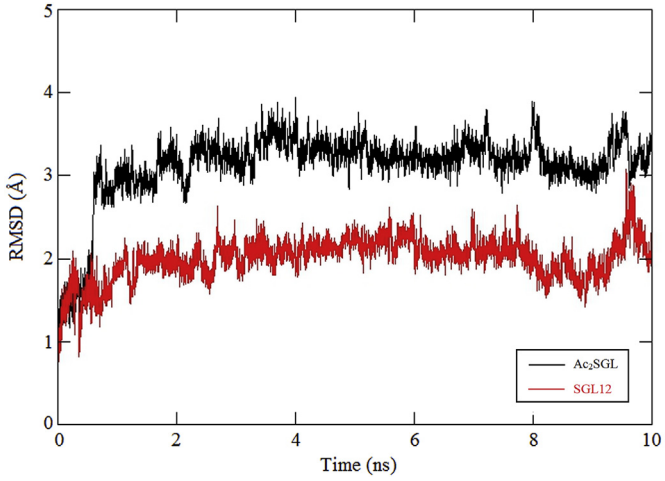

Fig. 3. Root mean square deviations (RMSD) of Ac_2SGL/SGL12 in complex with CD1b from molecular dynamics simulation. The all atom RMSD of Ac_2SGL and SGL12 was calculated from the starting structure and crystal structure, respectively.

Table 1
MMPBSA/GBSA free energy calculation of Ac_2SGL and SGL12 with CD1b.

Free energy method	Distribution	Ac_2SGL	SGL12
PBSA	vdW	−91.2 ± 5.2	−90.1 ± 4.2
	EEL	30.7 ± 13.9	71.6 ± 3.4
	EPB	−22.3 ± 10.6	−61.2 ± 2.1
	ENPOLAR	−9.4 ± 00.2	−12.1 ± 0.2
	ΔG gas	−69.2 ± 12.3	−18.6 ± 3.9
	ΔG solv	−29.3 ± 10.6	−73.3 ± 2.1
	ΔG Total	−98.5 ± 5.1	−91.9 ± 3.4
GBSA	vdW	−96.3 ± 5.2	−90.1 ± 4.2
	EEL	54.2 ± 27.8	143.1 ± 6.8
	EGB	−38.1 ± 20.9	−125.1 ± 3.8
	ESURF	−14.4 ± 0.6	−13.9 ± 0.2
	ΔG gas	−42.1 ± 25.7	53.0 ± 6.0
	ΔG solv	−52.5 ± 20.8	−139.0 ± 3.7
	ΔG Total	−94.6 ± 7.1	−86.0 ± 3.5

ΔG gas = vdW + EEL; ΔG solv = EPB + ENPOLAR/ESURF; ΔG Total = ΔG gas + ΔG solv; ΔG Tol, total binding free energy calculated by MMPBSA/GBSA method; all component are in kcal/mol.

sequence of dAbκ11was then aligned with selected templates. A total of 100 models were generated using MODELLER 9.14 [23] and DOPE score was used to rank the models. The quality of the top ranked dAbκ11 models were evaluated with PROCHECK [24], VERIFY-3D [25] and WHAT-IF [26]. The antibody binding site was predicted by Paratome [27].

2.5. Docking of dAbκ11 with lipid:CD1b (protein-protein docking)

The docking simulation of dAbκ11 with lipid:CD1b was performed using ZDOCK 3.0 [28]. Since dAbκ11 was reported to only bind to Ac_2SGL:CD1b complex [14], the non-CDRs and non-CD1b binding surfaces of dAbκ11 were blocked during the docking simulation. Clustering was performed using Kclust [29] and ranked using ZRANK [30]. The three top complexes were selected based on most dominant cluster and lowest ZRANK scoring. The complexes were then refined using RosettaDock [31] in local search refinement and rotamer library to generate another 1000 models. These 1000 models were re-ranked using ZRANK and the best complex was selected based on ZRANK and RosettaDock scoring function.

2.6. Molecular mechanic Poisson Boltzmann surface area/generalized born surface area (MMPBSA/GBSA) binding free energy calculation of lipid:CD1b with dAbκ11

Docked complexes of lipid:CD1b with dAbκ11 obtained from docking simulation were further sampled with molecular dynamics simulation. A similar preparation method of AMBER Protocol was used in dAbκ11 with lipid:CD1b refinement. The difference in preparation for the complex was that Cl^- ions were used to neutralise the overall charges. Then, similar minimisations for restrained complex at 300 kcal/mol/$Å^2$ and unrestrained minimization were used. In heating stage, the complex was gradually heated from 0 to 310 K within 20 ps by Langevin thermostat, while restrained with 100 kcal/mol/$Å^2$ for protein backbone, lipid and spacer. A 0.5 ns unrestrained MD simulation was performed to obtain constant pressure with equilibrated density at 310 K. The MD simulation was carried out for 10 ns. A total of 500 snapshots from the last 0.5 ns of MD simulation were used to calculate the binding free energy of lipids (Ac_2SGL & SGL12) with CD1b using the MMPBSA/GBSA method [32].

2.7. ELISA. Recognition of Ac_2SGL/SGL12:CD1b complexes by dAbκ11

Ac_2SGL, its synthetic analogue SGL12 (C24-tetramethylated fatty acid) and human sulphatide sulfoglycolipid (hSulf) (Avantis Polar Lipids, USA) were complexed in solution with recombinant human CD1b (Ac_2SGL:CD1b, SGL12:CD1b, hSulf:CD1b, respectively) [33].

A 96-well Maxisorp microplate (Nunc, USA) was coated (16 h/4 °C) with: **a)** BCD1b3.1 (anti-CD1b mAb), in order to capture CD1b complexes (Ac_2SGL:CD1b, SGL12:CD1b, hSulf:CD1b) and free CD1b and **b)** CD1e20.6 (anti-CD1e mAb) in order to capture recombinant human CD1e [34]. Both mAb were diluted on Carbonate-Bicarbonate pH 9.6 coating buffer (3 μg/mL). The plate was blocked with 3% PBS-skim milk (1 h/RT). Two washes (PBS-tween-20, 0.05%) were performed and Ac_2SGL:CD1b, SGL12:CD1b, hSulf:CD1b complexes, free CD1b and CD1e were added in PBS pH7.4 (1 μg/mL). After 3 washes (PBS-tween-20, 0.05%), dAbκ11 [14], diluted in 3% PBS-skim milk (10^8 phages) was added and the plate was incubated (1 h/RT). Subsequently, 3 washes were performed and HRP/Anti-M13 Monoclonal Conjugate (GE, Heathcare, Life Sciences) (diluted 1:5000 in 3% PBS-skim milk) was added. One hour later, the plate was washed as above, TMB liquid substrate (Sigma, USA) was added and incubated (10 min/RT). The reaction was stopped with 1M sulfuric acid (Merck, Germany) and absorbance (450 nm) was determined in a microplate reader (BioRad, USA). Each sample was studied in triplicate and the experiment was repeated three times.

2.8. Statistical analysis

Analysis of variance (ANOVA) was performed to compare Abs values and the Tukey multiple comparisons test was then performed to determine significant differences in the recognition of lipid:CD1b complexes by dAbκ11. Statistical analyses were performed using the GraphPad Prism version 4.0 software package for Windows (San Diego California, USA).

3. Results and discussion

3.1. Docking of lipid into CD1b

The docking of SGL12 into CD1b was used as the control to evaluate the suitability of our docking protocol and selected parameters. Docked SGL12 produced the binding conformation of root mean square deviation (RMSD) of 2.7 Å with the crystal structure (PDB id: 3T8X; Fig. 2a and b). In general, a good control docking should have RMSD of less than 2.0 Å [35]. However, as SGL12 has 50 rotatable bonds and that the alkyls tails are highly flexible, the RMSD value of 2.7 Å should be

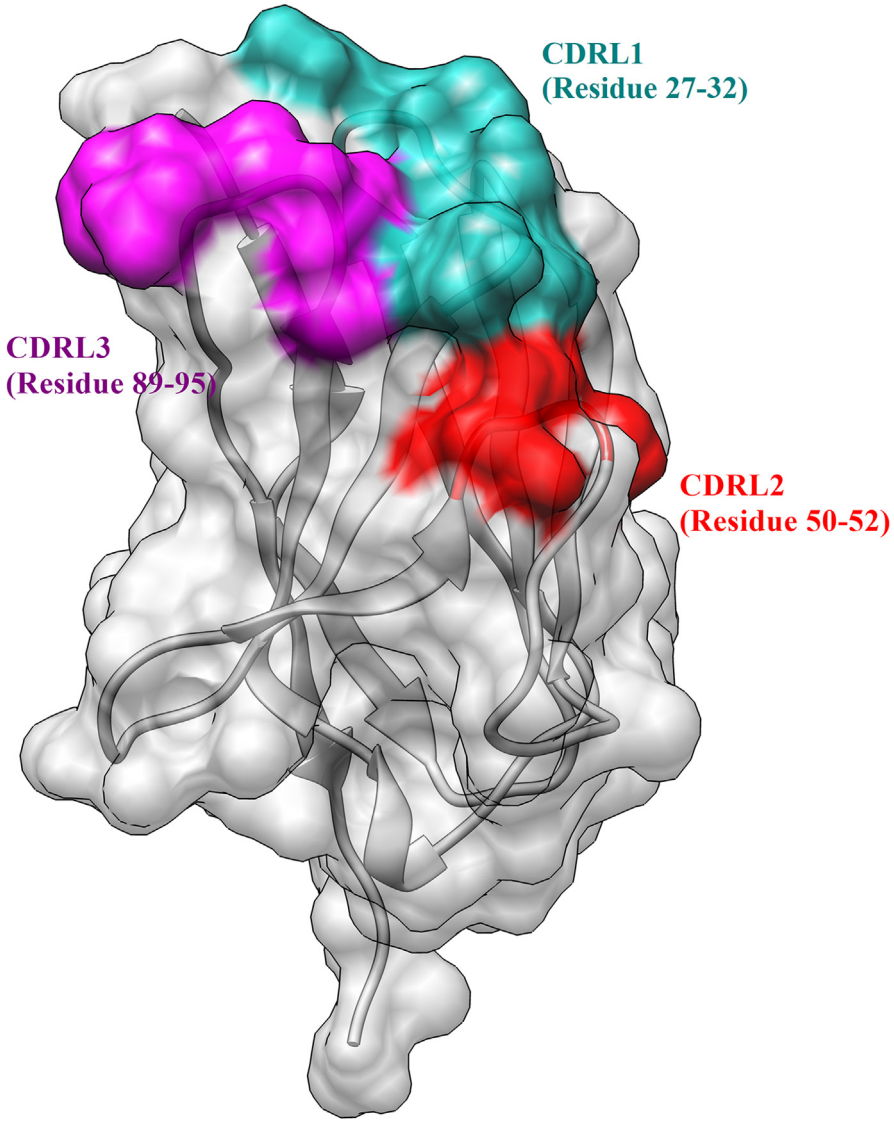

Fig. 4. Grey ribbon and surface presentation of dAbκ11 model from comparative modelling. Green, red and purple surface represent CDRL1, CDRL2 and CDRL3, respectively. The template 3UPA and 2BX5 is in yellow and blue ribbon representation, respectively. (For interpretation of the references to colour in this figure legend, the reader is referred to the Web version of this article.)

considered acceptable. In addition, to mimic the lipid loading into the CD1b protein, the spacer was included in the docking simulation. Spacer is a long hydrocarbon chain that is presented inside CD1b. This endogenous ligand is supposed to contribute to the overall structural stability and to participate in the control of antigen/lipid loading at late endosomes [13,27]. The presence of this spacer was proposed to prevent full-embedding of SGL12 within the protein groove, and thus to result in the exposure of the methyl branches from the phthioceranoyl-like tail outside the groove. These observations suggested that methyl motifs could be major determinants for T-cell recognition [13], something proven by investigations with many other synthetic analogues [11,12]. Thus, methyl branches of the longer tail of Ac_2SGL are expected to remain more revealed on the surface of CD1b. The hydrophilic SGL would therefore be positioned above the binding groove. In SGL12:CD1b crystal structure (PDB id: 3T8X), guanidinium group of Arg79 formed hydrogen bonding with the SGL12 sulphate glucose O_{10} and O_{11} (see atom numeration in Fig. 1) and held the disposition of the polar head in the CD1b surface, in agreement with the importance of this antigenic elements for T cell stimulation [10]. The docked SGL12 used as control showed similar hydrogen bonding with CD1b. Docked Ac_2SGL also has similar binding conformation of alkyl tails and trehalose sulphate with the crystal structure of SGL12 (Fig. 2c). A hydrogen bond was observed between CD1b Arg79 H_{N21} with Ac_2SGL O_{11} at the distance of 2.4 Å, which could also stabilise the Ac_2SGL sulphate head on the CD1b molecule.

SGL12:CD1b and Ac_2SGL:CD1b complexes obtained from the docking simulation were further studied with MD simulation. Ac_2SGL molecule (Fig. 3) showed a constant all atoms fluctuation at RMSD (from the starting structure) of ~3 Å after 1 ns. SGL12 has slightly lower RMSD value which is ~2 Å compared with the crystal structure. This thus indicated the conformational consistency of both Ac_2SGL and SGL12 docked models. Free binding energy calculations using MMPBSA/GBSA method showed that Ac_2SGL has slightly higher binding affinity (ΔG Total) with that of SGL12 (Table 1). However, binding affinities estimated with MMPBSA/GBSA methods could be overestimated, as indeed has also been reported in PDLD/s-LRA/β study [36–39]. The choice of the dielectric constant for theoretical simulation is a non-resolved long debate. Higher dielectric constants ($\varepsilon_{in} > 1$) are often preferred to treat highly charged binding interfaces [40,41]. Due to the low hydrophilic binding interface of lipids, the dielectric constant of 1 was used in this work.

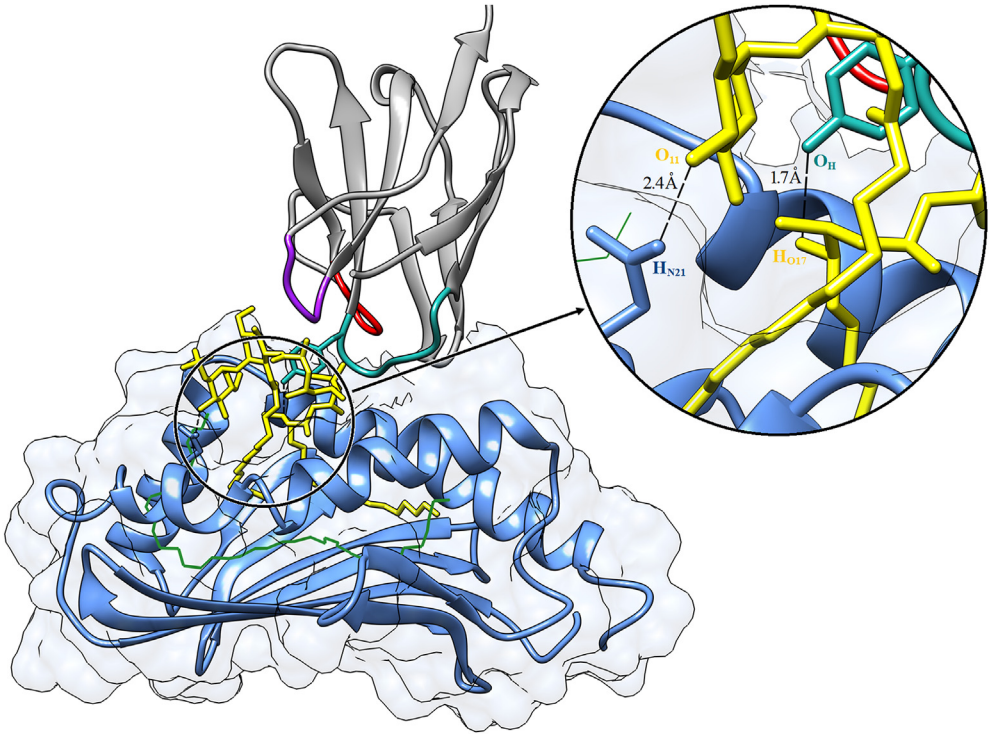

Fig. 5. The binding conformation of dAbκ11 (grey ribbon presentation; green ribbon is CDRL1, red ribbon is CDRL3 and maroon ribbon is CDRL3) with Ac_2SGL:CD1b (yellow stick is Ac_2SGL, blue ribbon and surface is CD1b, green line is spacer). The two black dotted lines in the close up circle are the hydrogen bonding of dAbκ11 Tyr32 O_H with Ac_2SGL H_{O17} and CD1b Arg79 H_{N21} with Ac_2SGL O_{11}. (For interpretation of the references to colour in this figure legend, the reader is referred to the Web version of this article.)

Table 2
MMPBSA/GBSA free energy calculation of dAbκ11 with lipid:CD1b.

Free energy method	Distribution	Ac_2SGL:CD1b	SGL12:CD1b
PBSA	vdW	−65.8 ± 4.4	−23.3 ± 3.4
	EEL	−87.2 ± 8.3	−67.7 ± 6.0
	EPB	101.7 ± 7.1	56.9 ± 2.9
	ENPOLAR	−10.0 ± 0.4	−3.7 ± 0.3
	ΔG gas	−152.9 ± 9.0	−91.1 ± 4.8
	ΔG solv	91.7 ± 6.9	53.1 ± 2.9
	ΔG Total	−61.2 ± 4.4	−37.9 ± 6.3
GBSA	vdW	−65.8 ± 4.4	−23.3 ± 3.4
	EEL	−174.3 ± 16.5	−135.4 ± 12.0
	EGB	209.8 ± 13.5	154.1 ± 9.0
	ESURF	−9.9 ± 0.6	−3.9 ± 0.3
	ΔG gas	−240.1 ± 16.7	−158.8 ± 10.3
	ΔG solv	200.0 ± 13.2	150.1 ± 9.0
	ΔG Total	−40.1 ± 5.5	−8.9 ± 2.7

ΔG gas = vdW + EEL; ΔG solv = EPB + ENPOLAR/ESURF; ΔG Total = ΔG gas + ΔG solv; ΔG Tol, total binding free energy calculated by MMPBSA/GBSA method; all component are in kcal/mol.

3.2. The model of dAbκ11

The CDRs of dAbκ11 are residues 27–32 (L1), 50–52 (L2) and 89–95 (L3) (Fig. 4). The quality of the dAbκ11 built model was evaluated using Ramachandran plot and results showed that 93.7% of the residues were in favourable regions (Supplementary Fig. S1a), with 0.08 Q-mean score (Supplementary Fig. S1b). The side chain compatibility evaluated by VERIFY-3D showed that 99.1% of dAbκ11 residues have scores above 0.2 (Supplementary Fig. S1c) and the packing quality control by WHAT-IF showed that 96.4% of the residues were above −5.0 (Supplementary Fig. S1d).

3.3. Docking of dAbκ11 with CD1b:SGL12/Ac_2SGL complexes

The initial docking search for dAbκ11 with SGL12/Ac_2SGL:CD1b complexes were predicted using ZDOCK. ZDOCK uses Fast Fourier algorithm to search for docking possess of dAbκ11 against CD1b:SGL12/

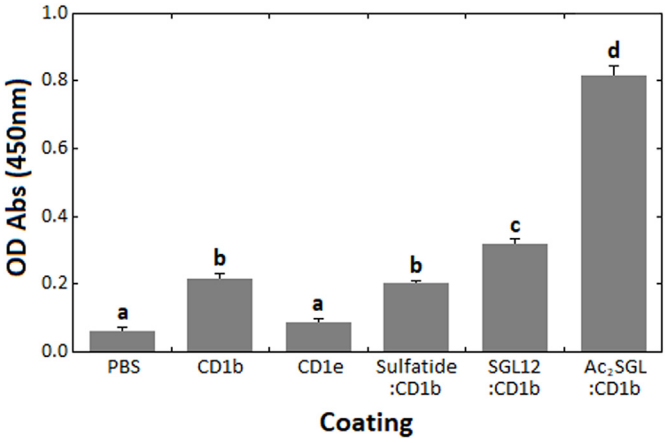

Fig. 6. ELISA results. Recognition of Ac2SGL:CD1b and CD1b:SGL12 complexes by dAbk11. The Ac2SGL:CD1b and SGL12:CD1b complexes were incubated in wells previously coated with the anti-CD1b mAb (BCD1b3.1). After incubation with the phage suspension (10^8 phage/mL), bound phages were detected with HRP/anti-M13 conjugate. Wells coated with BCD1b3.1 to capture CD1b and CD1b-sulphatide, as well as CD20.6 to capture CD1e, were used as negative controls. Data are plotted as the means of Abs values of three replicates ± SD. ANOVA and Tukey's test were used to compare Abs values. Different letters (a, b, c, d) means significant differences.

Ac_2SGL. The atomic positions of non-CDR and non-binding CD1b residues were restrained to reduce the search space. The first 2000 decoys were generated and clustered by ZDOCK. The decoys binding results were then re-clustered again at 5 Å RMSD using Kclust. Dominant clusters were then ranked by ZRANK. Three largest dominant clusters displaying the highest binding energy score from ZRANK were selected for the next step. RosettaDock was then used to refine the side chain of dAbκ11 by using the side-chain rotamers to improve the binding with SGL12/Ac_2SGL:CD1b. The joint use of ZDOCK and RosettaDock as docking tools was made to explore and search the most suitable docked model [31].

ZRANK results showed that dAbκ11 has a better binding energy

with Ac_2SGL:CD1b (−34.0 kcal/mol) than CD1b:SGL12 (−29.4 kcal/mol) even though both lipids have similar binding conformation. Only one hydrogen bond was observed between dAbκ11 Tyr32 O_H and Ac_2SGL H_{O17} in complex with CD1b (Fig. 5). The hydrogen bond distance of 1.7 Å indicated a strong interactions of dAbκ11 with Ac_2SGL:CD1b.

3.4. The interactions of dAbκ11 with CD1b:SGL12/Ac_2SGL complexes

The sulphate moiety of SGL is necessary for T-cell activation [10]. In addition, considering that the activation of the TCR is more prominent with Ac_2SGL compared to SGL12, therefore the acyl appendages could also be an important element for antigen recognition. In the observation, hydrogen bond was formed between dAbκ11 Tyr32 and Ac_2SGL hydroxyl acyl. This bond could only be established with CD1b:Ac_2SGL complex, as SGL12 does not have the hydroxyl compared with Ac_2SGL (Fig. 1).

The formation of a small hydrophobic groove between CDR1 and CDR3 was observed. Non-polar residues i.e. Ile 29, Ala 92 and Ala 93 formed hydrophobic contacts with methyl branches of Ac_2SGL, which were revealed above the CD1b groove. The extra methyl branches and the presence of hydroxyls on the acyl tail in Ac_2SGL has thus explained the better energetic terms that contribute to the higher specificity of dAbκ11 with Ac_2SGL than that of SGL12 [42].

The MMPBSA/GBSA binding free energy values showed that dAbκ11 has more favourable binding with CD1b:Ac_2SGL compared to SGL12:CD1b, despite both lipids have the same sugar moiety (Table 2). The binding of dAbκ11 with Ac_2SGL:CD1b further supported the theory of specificity of TCR recognition including interactions with CD1b as well as with Ac_2SGL [43]. The major contributions of the binding were the electrostatic interactions (EEL) followed by van der Waals (vdW) interactions (Table 2).

This computational study has enabled the better understanding on the preference of dAbκ11 towards CD1b:Ac_2SGL rather than SGL12:CD1b at the molecular level. However, in order to further study and explain the obtained results, a mutation scanning on the dAbκ11 CDRs might useful to provide additional evaluation. This can also be carried out together with pairwise decomposition calculation in order to identify hotspot residues of dAbκ11 for the future design of dAbκ11 analogues.

3.5. In vitro recognition of Ac_2SGL/SGL:CD1b complexes by dAbκ11

From ELISA results, a significant higher recognition ($p < 0.001$) of dAbκ11 was showed for Ac_2SGL:CD1b and SGL12:CD1b complexes than for all other targets (Fig. 6). However, the recognition of Ac_2SGL:CD1b by dAbκ11 was much higher compared to SGL12:CD1b ($p < 0.001$). The dAbκ11 showed higher recognition of CD1b and CD1b-sulfatide complex compared to CD1e and PBS ($p < 0.001$), which could represent some degree of recognition of the antigen presenting molecule. The results of the evaluation of the binding capacity of dAbk11 to CD1b complexed with Ac_2SGL or its synthetic analogue SGL12 are in concordance with the results from the modelling experiment, which predicted a similar behaviour of dAbk11 against the two complexes. It is important to note that dAbk11 was obtained with the use of a human synthetic phage antibody library, using as a target for the panning process THP1 cells expressing human CD1b complexed with the natural sulphoglycolipid, Ac_2SGL, and not with a synthetic analogue [14]. This fact could justify the preferential recognition of the CD1b complexed with Ac_2SGL by dAbk11.

A similar result was obtained with a single-chain TCR produced from the TCR of a human T cell clone recognizing the Ac_2SGL:CD1b complex, where the recognition of Ac_2SGL:CD1b was more prominent compared to SGL12:CD1b [44]. Regarding the results of the modelling, although the ELISA results are not a direct validation of the mechanism suggested by the simulation, they were qualitatively compatible with the prediction.

4. Conclusions

A better binding affinity of dAbκ11 with CD1b:Ac_2SGL than CD1b:SGL12 was observed from theoretical simulations. Free energy calculation showed that the interactions of dAbκ11 with Ac_2SGL:CD1b are mainly contributed by van der Waals and electrostatic forces. A rather strong hydrogen bond with 1.7 Å distance was formed between dAbκ11 Tyr32 O_H and Ac_2SGL H_{O17} in complex with CD1b. The ability of dAbκ11 to discriminate between CD1b complexes with the Mtb natural lipid Ac_2SGL and synthetic SGL12 at molecular level was also further supported by the experimental ELISA results. The results obtained could further the possible optimization of dAbk11 to enhance the binding with CD1b:Ac_2SGL for future applications.

Conflicts of interest

The authors declare that they have no competing interest.

Acknowledgments

This work was funded by Fundamental Research Grant Scheme (FRGS; 203/CIPPM/6711439), Higher Institution Centre of Excellence Grant (HICoE; 311/CIPPM/44001005) and LRGS Grant, (203/PPSK/67212002) from Ministry of Education Malaysia. Thanks also to Graduate Assistant Scheme from Universiti Sains Malaysia and MyBrain MyMaster from Malaysia Ministry of Higher Education for C.T. Law.

Appendix A. Supplementary data

Supplementary data to this article can be found online at https://doi.org/10.1016/j.tube.2018.11.002.

References

[1] Marais BJ, Lönnroth K, Lawn SD, Migliori GB, Mwaba P, Glaziou P, Bates M, Colagiuri R, Zijenah L, Swaminathan S, Memish ZA, Pletschette M, Hoelscher M, Abubakar I, Hasan R, Zafar A, Pantaleo G, Craig G, Kim P, Maeurer M, Schito M, Zumla A. Tuberculosis comorbidity with communicable and non-communicable diseases: integrating health services and control efforts. Lancet Infect Dis 2013;13:436–48.

[2] Zumla A, George A, Sharma V, Herbert N. WHO's 2013 global report on tuberculosis: successes, threats, and opportunities. Lancet 2013;382:1765–7.

[3] Zumla A, Raviglione M, Hafner R, von Reyn CF. Tuberculosis. N Engl J Med 2013;368:745–55.

[4] Falzon D, Raviglione MC. TB control: achievements, obstacles and the role of vaccines. In: Norazmi MN, Acosta A, Sarmiento ME, editors. The art and science of tuberculosis vaccine development. Shah Alam: Oxford University Press; 2014. p. 13–29.

[5] Hermans S, Horsburgh Jr. CR, Wood R. A century of tuberculosis epidemiology in the Northern and Southern Hemisphere: the differential impact of control interventions. PloS One 2015;10:e0135179.

[6] Dye C, Glaziou P. The global tuberculosis epidemic: scale, dynamics, and prospects for control. In: Raviglione MC, editor. Tuberculosis: the essentials. Boca Raton: CRC Press; 2016. p. 1–22.

[7] Geadas C, Stoszek SK, Sherman D, Andrade BB, Srinivasan S, Hamilton CD, Ellner J. Advances in basic and translational tuberculosis research: proceedings of the first meeting of RePORT international. Tuberculosis (Edinb) 2017;102:55–67.

[8] Somnay-Wadgaonkar K, Nusrat A, Kim HS, Canchis WP, Balk SP, Colgan SP, Blumberg RS. Immunolocalization of CD1d in human intestinal epithelial cells and identification of a β2-microglobulin-associated form. Int Immunol 1999;11:383–92.

[9] Moody DB, Zajonc DM, Wilson IA. Anatomy of CD1-lipid antigen complexes. Nat Rev Immunol 2005;5:387–99.

[10] Gilleron M, Stenger S, Mazorra Z, Wittke F, Mariotti S, Bohmer G, Prandi J, Mori L, Puzo G, De Libero G. Diacylated sulfoglycolipids are novel mycobacterial antigens stimulating CD1-restricted T cells during infection with *Mycobacterium tuberculosis*. J Exp Med 2004;199:649–59.

[11] Guiard J, Collmann A, Garcia-Alles LF, Mourey L, Brando T, Mori L, Gilleron M, Prandi J, De Libero G, Puzo G. Fatty acyl structures of *Mycobacterium tuberculosis*-sulfoglycolipid govern T cell response. J Immunol 2009;182:7030–7.

[12] Gau B, Lemetais A, Lepore M, Garcia-Alles LF, Bourdreux Y, Mori L, Gilleron M, De Libero G, Puzo G, Beau JM, Prandi J. Simplified deoxypropionate acyl chains for *Mycobacterium tuberculosis* sulfoglycolipid analogues: chain length is essential for high antigenicity. Chembiochem 2013;14:2413–7.

[13] Garcia-Alles LF, Collmann A, Versluis C, Lindner B, Guiard J, Maveyraud L, Huc E, Im JS, Sansano S, Brando T, Julien S, Prandi J, Gilleron M, Porcelli SA, de la Salle H, Heck AJ, Mori L, Puzo G, Mourey L, De Libero G. Structural reorganization of the antigen-binding groove of human CD1b for presentation of mycobacterial sulfoglycolipids. Proc Natl Acad Sci U S A 2011;108:17755–60.
[14] Camacho F, Sarmiento ME, Reyes F, Kim L, Huggett J, Lepore M, Otero O, Gilleron M, Puzo G, Norazmi MN. Selection of phage-displayed human antibody fragments specific for CD1b presenting the *Mycobacterium tuberculosis*glycolipid Ac 2 SGL. Int J Mycobacteriol 2016;5:120–7.
[15] Studio D. Version 3.0. San Diego, CA: Accelrys Software Inc.; 2010.
[16] Morris GM, Huey R, Lindstrom W, Sanner MF, Belew RK, Goodsell DS, Olson AJ. AutoDock 4 and AutoDockTools 4: automated docking with selective receptor flexibility. J Comput Chem 2009;30:2785–91.
[17] Trott O, Olson AJ. AutoDock Vina: improving the speed and accuracy of docking with a new scoring function, efficient optimization, and multithreading. J Comput Chem 2010;31:455–61.
[18] Case DA, Darden TA, Cheatham III TE, Simmerling CL, Wang J, Duke RE, Luo R, Walker RC, Zhang W, Merz KM. AMBER 12. San Francisco. 2012.
[19] Kabat EA, Te Wu T, Perry HM, Gottesman KS, Foeller C. Sequences of proteins of immunological interest. Bethesda: National Institutes of Health; 1992.
[20] Altschul SF, Madden TL, Schäffer AA, Zhang J, Zhang Z, Miller W, Lipman DJ. Gapped BLAST and PSI-BLAST: a new generation of protein database search programs. Nucleic Acids Res 1997;25:3389–402.
[21] James LC, Jones PC, McCoy A, Tennent GA, Pepys MB, Famm K, Winter G. β-edge interactions in a pentadecameric human antibody Vκ domain. J Mol Biol 2007;367:603–8.
[22] Dudgeon K, Rouet R, Kokmeijer I, Schofield P, Stolp J, Langley D, Stock D, Christ D. General strategy for the generation of human antibody variable domains with increased aggregation resistance. Proc Natl Acad Sci USA 2012;109:10879–84.
[23] Webb B, Sali A. Comparative protein structure modeling using Modeller. Curr Protoc Bioinform 2014;5:6.1–5.6.32.
[24] Laskowski RA, MacArthur MW, Moss DS, Thornton JM. PROCHECK: a program to check the stereochemical quality of protein structures. J Appl Crystallogr 1993;26:283–91.
[25] Luthy R, Bowie JU, Eisenberg D. Assessment of protein models with three-dimensional profiles. Nature 1992;356:83–5.
[26] Vriend G, Sander C. Quality control of protein models: directional atomic contact analysis. J Appl Crystallogr 1993;26:47–60.
[27] Kunik V, Ashkenazi S, Ofran Y. Paratome: an online tool for systematic identification of antigen-binding regions in antibodies based on sequence or structure. Nucleic Acids Res 2012;40:W521–4.
[28] Chen R, Li L, Weng Z. ZDOCK: an initial-stage protein-docking algorithm. Proteins Struct Func Bioinf 2003;52:80–7.
[29] Hauser M, Mayer CE, Söding J. kClust: fast and sensitive clustering of large protein sequence databases. BMC Bioinf 2013;14:1.
[30] Pierce B, Weng Z. ZRANK: reranking protein docking predictions with an optimized energy function. Proteins 2007;67:1078–86.
[31] Pierce B, Weng Z. A combination of rescoring and refinement significantly improves protein docking performance. Proteins: Struct Func Bioinf 2008;72:270–9.
[32] Massova I, Kollman PA. Combined molecular mechanical and continuum solvent approach (MM-PBSA/GBSA) to predict ligand binding. Perspect Drug Discov 2000;18:113–35.
[33] Garcia-Alles LF, Versluis K, Maveyraud L, Vallina AT, Sansano S, Bello NF, Gober HJ, Guillet V, de la Salle H, Puzo G, Mori L, Heck AJ, De Libero G, Mourey L. Endogenous phosphatidylcholine and a long spacer ligand stabilize the lipid-binding groove of CD1b. EMBO J 2006;25:3684–92.
[34] Mukherjee S, Balius TE, Rizzo RC. Docking validation resources: protein family and ligand flexibility experiments. J Chem Inf Model 2010;50:1986–2000.
[35] Mukherjee S, Balius TE, Rizzo RC. Docking validation resources: protein family and ligand flexibility experiments. J Chem Inf Model 2010;50:1986–2000.
[36] Warshel A. Computer modeling of chemical reactions in enzymes and solutions. New York: Wiley; 1991.
[37] Sham YY, Muegge I, Warshel A. The effect of protein relaxation on charge-charge interactions and dielectric constants of proteins. Biophys J 1998;74:1744–53.
[38] Schutz CN, Warshel A. What are the dielectric "constants" of proteins and how to validate electrostatic models? Proteins: Struct Func Bioinf 2001;44:400–17.
[39] Genheden S, Ryde U. The MM/PBSA and MM/GBSA methods to estimate ligand-binding affinities. Expet Opin Drug Discov 2015;10:449–61.
[40] Hou T, Wang J, Li Y, Wang W. Assessing the performance of the MM/PBSA and MM/GBSA methods. 1. The accuracy of binding free energy calculations based on molecular dynamics simulations. J Chem Inf Model 2011;51:69–82.
[41] Kržan M, Vianello R, Maršavelski A, Repič M, Zakšek M, Kotnik K, Fijan E, Mavri J. The quantum nature of drug-receptor interactions: deuteration changes binding affinities for histamine receptor ligands. PloS One 2016;11:e0154002.
[42] Chowell D, Krishna S, Becker PD, Cocita C, Shu J, Tan X, Greenberg PD, Klavinskis LS, Blattman JN, Anderson KS. TCR contact residue hydrophobicity is a hallmark of immunogenic CD8+ T cell epitopes. Proc Natl Acad Sci USA 2015;112:1754–62.
[43] Grant EP, Beckman EM, Behar SM, Degano M, Frederique D, Besra GS, Wilson IA, Porcelli SA, Furlong ST, Brenner MB. Fine specificity of TCR complementarity-determining region residues and lipid antigen hydrophilic moieties in the recognition of a CD1-lipid complex. J Immunol 2002;168:3933–40.
[44] Camacho F, Huggett J, Kim L, Infante JF, Lepore M, Perez V, Sarmiento ME, Rook G, Acosta A. Phage display of functional alphabeta single-chain T-cell receptor molecules specific for CD1b:Ac(2)SGL complexes from *Mycobacterium tuberculosis*-infected cells. BMC Immunol 2013;14(Suppl 1):S2.